

We are IntechOpen, the world's leading publisher of Open Access books Built by scientists, for scientists

6,900

Open access books available

186,000

International authors and editors

200M

Downloads

Our authors are among the

154

Countries delivered to

TOP 1%

most cited scientists

12.2%

Contributors from top 500 universities



WEB OF SCIENCE™

Selection of our books indexed in the Book Citation Index
in Web of Science™ Core Collection (BKCI)

Interested in publishing with us?
Contact book.department@intechopen.com

Numbers displayed above are based on latest data collected.
For more information visit www.intechopen.com



Broadband Complex Permittivity Determination for Biomedical Applications

Radim Zajíček and Jan Vrba
Czech Technical University in Prague, Dept. of Electromagnetic Field, FEE
Czech Republic

1. Introduction

Medicine has the essential profit from microwave technique such as not only a development of new devices but also an improvement of existing devices. Generally, we want to *Look and See* using microwaves in the medical diagnostics and imaging and to *Heat and Destroy* in the medical therapy. But also the non-thermal effects of electromagnetic fields have a serious part in studying the biological effects of electromagnetic fields.

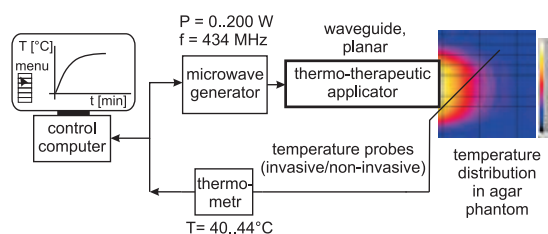


Fig. 1. Therapeutic Application of Microwave Technique: Microwave Hyperthermia

A knowledge of the dielectric parameters of materials is important for microwave or radio engineers involved in the analysis and synthesis of devices. Relative permittivity, loss factor and conductivity are the input parameters for electromagnetic field modelling and simulations. Although for many materials these parameters can be found in the tables, their experimental determination is very often necessary.

1.1 Applications of Microwaves in Medicine

The dielectric properties of biological tissues are the determining factors for the dissipation of electromagnetic energy in the human body and they are therefore the basic parameters for hyperthermia cancer treatment (Fig. 1). The measurement of the dielectric parameters of biological tissues is also a promising method in medical diagnostics and imaging. Knowledge of the complex permittivity¹ in an area under treatment, i.e. knowledge of the complex permittivity of healthy and tumor tissue, is extremely important for example in diagnosing tumor cell-nests in the human body or in the design of thermo-therapeutic applicators which transform electromagnetic energy into thermal energy in pathological tissue (Vrba, 2003).

¹ Complex permittivity is also known as a dielectric constant in literature.

Let's summarize the basic characteristics of microwaves, their advantages and limitations, and applications in the medicine:

General characteristic:

- from 100 MHz to 30 GHz frequency range
- diagnostic applications: a tumor detection based on differences in the tissue electrical properties
- therapeutic applications: a treatment based on the local heating or the regional (whole-body) heating - hyperthermia integrated with MRI, prostate hyperplasia, heart and other tissue ablation, angioplasty
- other applications: radiometry, telemetry, motion detection

Advantages of microwaves:

- offer a wide frequency range
- an ability to focus the energy
- a variety of simulation tools (methods for field solving²)
- a relatively low cost of microwave components and devices
- a low if any health risk

Limitations of microwaves:

- a spatial resolution
- penetration depth of electromagnetic waves
- electromagnetic interferences

Summary of the human characteristics from microwave view point:

- differences in tissue properties (normal/tumor tissue, low/high water content)
- scattering of complex patterns of fields in the body
- individual anatomical differences

1.2 Complex permittivity

The complex permittivity is a quantity which describes the electrical properties of materials. In case of non-conductors, dielectrics, the complex permittivity describes an interaction between the dielectric and the applied external electric field.

Polarization

The interaction of an electric field with a biological tissue has the origin in the response of the charge particles to the applied field. The displacement of these charge particles from their equilibrium positions gives rise to induced dipoles which respond to the applied field. Such induced polarization arises mainly from the displacement of electrons around nuclei (electronic polarization) or due to the relative displacement of atomic nuclei because of the

² FEM - Finite Element Method is utilized mostly in frequency domain, body parts are represented by surfaces and volumes are divided into tetrahedrons. FDTD - Finite Difference in Time Domain utilized voxel representation of body tissues.

unequal distribution of charge in molecule formation (atomic polarization). In addition to induced dipoles some dielectrics, known as polar dielectrics, contain permanent dipoles due to the asymmetric charge distribution of unlike charge partners in a molecule which tend to reorientation under the influence of a changing electric field, thus giving rise to orientation polarization. Finally, another source of polarization arises from charge build-up in interfaces

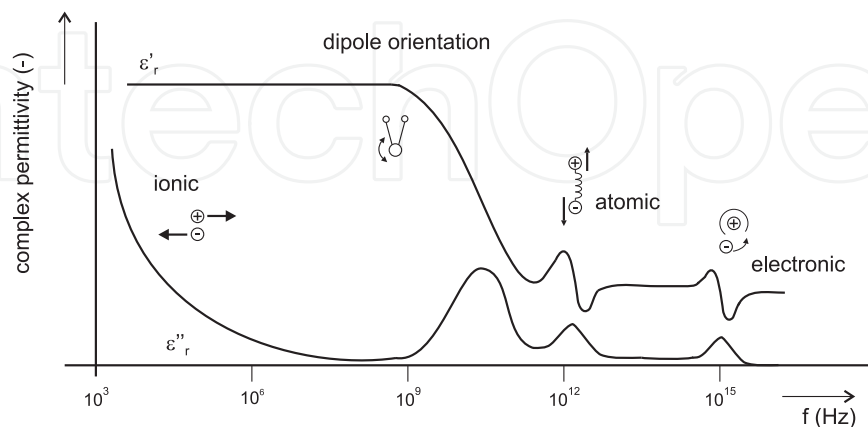


Fig. 2. Polarization effects at a broad frequency range

between components in heterogeneous systems, termed interfacial, space charge or Maxwell-Wagner polarization. The Maxwell-Wagner polarization and orientation polarization due to an alternating electric field together with d.c. conductivity are the basic of thermal effect of microwaves (Kittel, 1966).

Permittivity is known from the physics or theory of electromagnetic field as

$$\varepsilon = \varepsilon_0 \varepsilon_c \quad (1)$$

where ε_0 is free space permittivity and ε_c is complex relative permittivity (dielectrics are very often lossy). Complex relative permittivity can be given in turn as

$$\varepsilon_c = \varepsilon_r - j\varepsilon_r \tan \delta \quad (2)$$

where ε_r is a real part of complex relative permittivity³ and $\tan \delta$ is the loss factor. For purely conductive losses

$$\tan \delta = \frac{\sigma}{\omega \varepsilon_0 \varepsilon_r} \quad (3)$$

applies, where σ is the medium conductivity.

Derivation of Complex Permittivity

It would be helpful if, through some elementary analysis, the complex nature of permittivity is demonstrated without having to assume this premise from the start. Ampere's circuital law in its elementary form contains all the necessary components needed for this analysis. Maxwell modified Ampere's law by including a displacement current density term for sinusoidal electric field variations

$$\text{rot} \mathbf{H} = \mathbf{J} + j\omega \mathbf{D} \quad (4)$$

³ The real part of complex relative permittivity is very often called only relative permittivity. One must carefully consider where it is possible (for example for the simplification of terms) to reduce complex relative permittivity to only relative permittivity.

where \mathbf{H} is magnetic field strength, \mathbf{J} is current density, \mathbf{D} is electric flux density and t is time. The conduction current density is a function of the electric field vector (Ohm's law)

$$\mathbf{J} = \sigma \mathbf{E} \quad (5)$$

where σ is medium conductivity. Using material formula $\mathbf{D} = \epsilon \mathbf{E}$ and $\epsilon = \epsilon_0 \epsilon_r$ is

$$\text{rot} \mathbf{H} = \sigma \mathbf{E} + j\omega \epsilon_0 \epsilon_r \mathbf{E} = j\omega \epsilon_0 \mathbf{E} \left(\epsilon_r + \frac{\sigma}{j\omega \epsilon_0} \right) = j\omega \epsilon_0 \mathbf{E} \left(\epsilon_r - j \frac{\sigma}{\omega \epsilon_0} \right) \quad (6)$$

Complex relative permittivity is finally expressed

$$\epsilon_c = \epsilon_r' - j\epsilon_r'' = \epsilon_r - j \frac{\sigma}{\omega \epsilon_0} \quad (7)$$

1.3 Complex permittivity determinaton

A more or less extensive tabulation of the dielectric properties of materials selected to illustrate the theoretical deliberations provided by the authors is common to all papers in the field of complex permittivity measurement. Nowadays, papers are instigated for example by the need for such information for electromagnetic dosimetry. To date there is no consensus on the dielectric data (Gabriel, 1996).

Systems using complex permittivity measurement exist, and some are even commercially available (e.g. the Agilent Technologies 85070 analyzer) but the Czech Technical University in Prague is not equipped with this type of material measurement system. Our work is motivated by the need for cheap⁴ but accurate determination of the complex permittivity with the measurement technique which is also easy to manufacture and therefore would be interesting for many researchers.

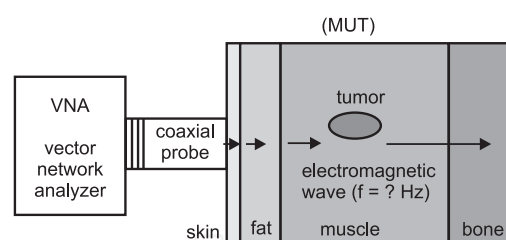


Fig. 3. This illustrates the principle of the reflection method - a medical diagnostics and imaging concept using microwaves. The different equivalent penetration depths of microwaves at different frequencies enable us to diagnose the tissues (layers) in the area under treatment.

2. Materials and Methods

There are several methods for measuring the complex permittivity - the resonance method, measurement in free space and the transmission line method (Fig. 4). If we want to use a broadband measurement method that is non-destructive and non-invasive, we should choose a reflection method on an open-ended coaxial line-a method based on the reflection coefficient measurement of an open-ended coaxial line attached to the sample of the measured dielectric.

⁴ The cost of mentioned Agilent system is \$5000 approximately, <http://www.agilent.com>.

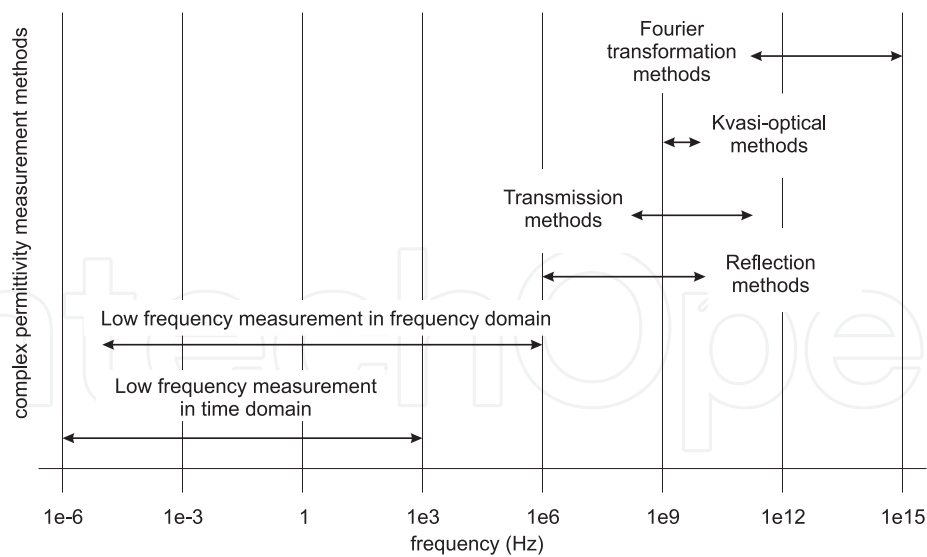


Fig. 4. Complex permittivity determination in a broad frequency band

2.1 Reflection Coefficient

Reflection coefficient relates the tangential components of the incident and the reflected electric fields and is a frequency dependent and complex quantity⁵

$$\Gamma = \frac{\mathbf{E}_r}{\mathbf{E}_i} \tag{8}$$

where \mathbf{E}_r is the reflected wave and \mathbf{E}_i is the incident wave (Novotný, 2005).

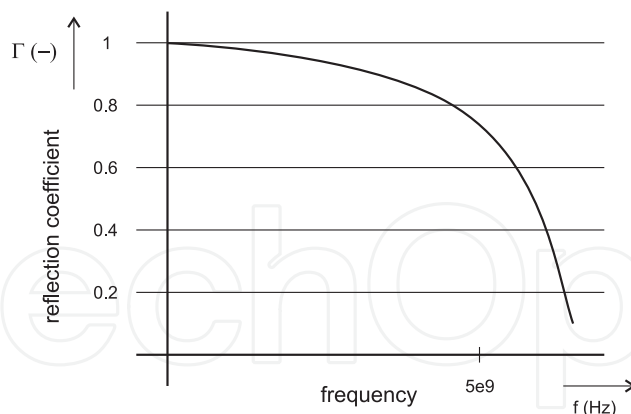


Fig. 5. Frequency behavior of the reflection coefficient

In case of interface between two materials with different impedances, the reflection coefficient is defined

$$\Gamma = \frac{Z_1 - Z_0}{Z_1 + Z_0} \tag{9}$$

⁵ It is important to note the reflection coefficient is a voltage quantity and it is related to a power quantity with the term $\Gamma_P \approx \Gamma^2$. It is possible to find the reflection coefficient as R , Γ or S_{11} in technical literature.

where Z_0 and Z_1 are impedances of materials-in described measurement technique the impedance of coaxial line is $Z_0 = 50 \Omega$ and the impedance of a MUT sample is Z_1 (generally complex impedance).

2.2 Relation between Reflection and Permittivity

The reflection method entails the measurement of the reflection coefficient on the interface between two materials, on the open end of the coaxial line (as a detector) and the material being tested (MUT, Fig. 6). It is a well-known method for determining dielectric parameters

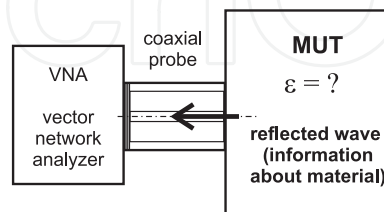


Fig. 6. Dielectric measurement from the viewpoint of electromagnetic field theory and wave propagation on the interface between the coaxial probe and the MUT

(Stuchly et al., 1982). This method is based on the fact that the reflection coefficient of an open-ended coaxial line depends on the dielectric parameters of the MUT that is attached to it. To calculate the complex permittivity from the measured reflection coefficient, it is useful to use an equivalent circuit of an open-ended coaxial line. Fig. 6 shows the complex permittivity measurement from the point of view of electromagnetic field theory and the propagation of the electromagnetic wave on the interface between two materials with different impedances (Novotný, 2001). The probe translates changes in the permittivity of a MUT into changes in the input reflection coefficient of the probe.

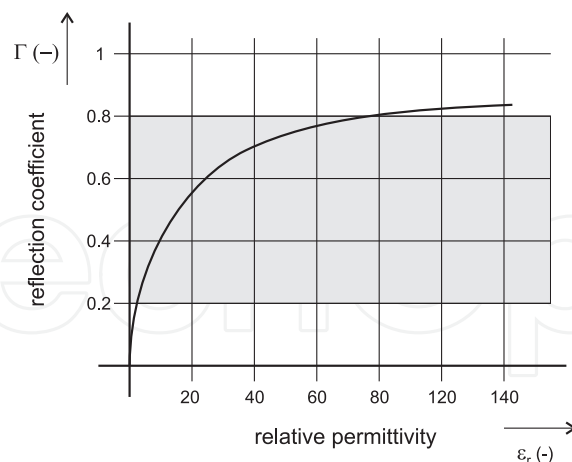


Fig. 7. Reflection coefficient versus relative permittivity

The reflection coefficient is varying a lot for the small values of relative permittivity (approximately less than 20, Fig. 7). Complex permittivity measurement is more sensitive and hence precise. Conversely, for high values of relative permittivity (for example between 70 and 90) there is a little change of the reflection coefficient and the measurement has more uncertainties.

The interface between the measurement probe and a MUT sample represents an impedance jump because of biological tissues have extremely high permittivity values. At low frequencies their permittivity can be more than 100 and the value of the loss factor more than 0.1. An accurate evaluation is very difficult because the reflection coefficient is close to 1 (Fig. 5). This means that only a very small part of the incident energy penetrates into the sample.

The surface of the sample of MUT must be in perfect contact with the probe. The thickness of a measured sample must be at least twice an equivalent penetration depth of the electromagnetic wave d . This ensures that the waves reflected from the far MUT interface are attenuated by approximately -35 dB, which assures that their effect on the measured reflection coefficient is insignificant.

$$d = \sqrt{\frac{2}{\omega\mu\sigma}} = \frac{1}{\omega} \sqrt{\frac{2}{\mu\varepsilon_0\varepsilon_r \tan \delta}} \quad (10)$$

The dependence of equivalent penetration depth d on dielectric parameters ε_r and $\tan \delta$ and also frequency f denotes Eq. 10. Typical values of d for distilled water and biological muscle tissue at different frequencies are summarized in Tab. 1.

Materials	f (MHz)	$2d$ (mm)
distilled water	434	71.2
	915	34.0
	2450	12.8
muscle tissue	434	25.9
	915	24.2
	2450	15.6

Table 1. Equivalent penetration depth of the electromagnetic wave into different materials: distilled water and muscle tissue

2.3 Coaxial Probes

When a wave has only transverse field components for both the electric and magnetic field and no longitudinal components ($E_z = 0$ and $H_z = 0$), the wave is transverse electromagnetic (TEM). Transverse electromagnetic waves are very much appreciated in practice because they

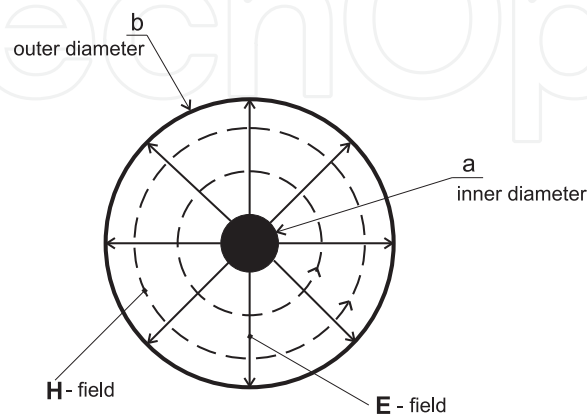


Fig. 8. Coaxial transmission line.

have only four components, with no longitudinal components. On the other hand, uniform plane waves also characterize a very simple structure. As an example, the very well known coaxial cable has a TEM wave as the main propagating mode (Fig. 8). The surface of constant phase is indeed a plane, perpendicular to the direction of propagation, hence the wave is planar. The field, however, is not constant over the plane because it varies between the two conductors according to a $1/r$ law. Hence, the TEM wave in a coaxial cable is a nonuniform plane wave.

N&SMA Connector Type Probe

N type coaxial connectors are medium size units which have constant 50Ω impedance and provide radio frequency performance up to 11 GHz. SMA (SubMiniature, version A) connectors are coaxial RF connectors developed as a minimal connector interface for coaxial cable with a screw type coupling mechanism. The connector has a 50Ω impedance. It offers excellent electrical performance from DC to 18 GHz.

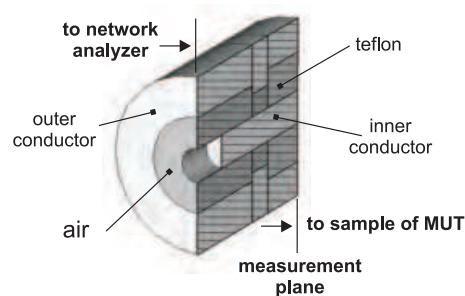


Fig. 9. Measurement coaxial probe: description and dimensions - inner/outer diameter: N connector type probe 3/7 mm, SMA connector type probe 1.3/4 mm

We have adapted the standard N and SMA connectors for this measurement method from which the parts for connecting to a panel were removed (Fig. 9). The measurement probe can be described by the equivalent circuit consisting of fringing capacitance between inner and outer conductor out of the coaxial structure and radiating conductance which represents propagation losses (Fig. 10). The capacitance and conductance are frequency and permittivity dependent and are also dependent on the dimensions (inner and outer diameters) of the probe.

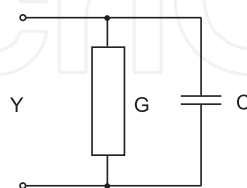


Fig. 10. An equivalent circuit of the open end of coaxial line: admittance of the probe Y has two components - fringing capacitance C and radiating conductance G

A measurement probe can be described as an antenna with the input admittance ($Y = G + jB$, where G is conductance and B is susceptance) expressed as

$$Y_0 = G_0(\epsilon_c, \omega) + j\omega C_0(\epsilon_c, \omega) \quad (11)$$

where C_0 and G_0 are constants if the antenna radiates in free space ($\epsilon_c = 1$).

If we change the free space surrounding the medium for a lossy biological tissue medium, the dependence of this antenna admittance on the properties of surrounding medium can be derived using Deschamps' theorem (Deschamps, 1962). Admittance changes - Y (in Eq. 12) is now an admittance of the antenna immersed in a medium of permittivity ϵ_c (Fig. 11)

$$Y(\epsilon_c, \omega) = \sqrt{\epsilon_c} Y_0(1, \omega \sqrt{\epsilon_c}) \tag{12}$$

This means that the admittance of medium of permittivity ϵ_c at angular frequency ω is the same as the admittance measured in the free space at frequency $\sqrt{\epsilon_c}$ -times higher furthermore multiplied by $\sqrt{\epsilon_c}$.

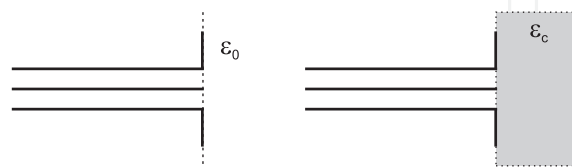


Fig. 11. Illustration to the principle of Deschamps' Theorem: a coaxial probe radiates into free space and then into the lossy medium

The capacitance C_0 can be considered to be a constant (in free space). The radiation into the dielectric surrounding the antenna can be calculated when the dielectric is air (Liu, 1986). Expanding the Bessel function into a Maclaurin series yields

$$G_0 = \frac{Y_0}{\ln \frac{a}{b}} \int_{\pi/2}^0 [J_0(ka \sin \Theta) - J_0(kb \sin \Theta)]^2 \frac{d\Theta}{\sin \Theta} \tag{13}$$

$$\approx \frac{Y_0}{\ln \frac{a}{b}} [G_1(f^4) + G_2(f^6) + \dots] \tag{14}$$

where $J_0(x)$ is the Bessel function and G_i are parameters dependent on the antenna dimensions (radius a and b) and wavelength. An investigation of coefficients G_i showed that $G \approx G_1$ for the N and SMA connector type probes. Therefore the radiation effect of coaxial probe, which is represented as radiation conductance in the probe's equivalent circuit, can be approximate as varying with frequency f^4

$$G_1(f^4) = \frac{2}{3} (a^2 - b^2) \frac{\pi^4}{c^4} f^4 \approx f^4 \tag{15}$$

Let us apply Deschamps' theorem - Eq. 12 to Eq. 11

$$Y_0 = G_0 + j\omega C_0 \Leftrightarrow Y(\omega, \epsilon_c) = \sqrt{\epsilon_c} G_0 (\sqrt{\epsilon_c})^4 + \sqrt{\epsilon_c} j\omega C_0 \sqrt{\epsilon_c} \tag{16}$$

The input admittance of the coaxial transmission line as the antenna in a lossy dielectric is then

$$Y = \sqrt{\epsilon_c^5} G_0 + j\omega \epsilon_c C_0 \tag{17}$$

where, with respect to the measurement, Y is the measured admittance of the probe, C_0 and G_0 are constants given by the equivalent circuit of the probe in free space (Fig. 10).

Admittance Y is related to the measured reflection coefficient S_{11}

$$Y = Y_0 \frac{1 - S_{11}}{1 + S_{11}} \quad (18)$$

where $Y_0 = 1/(50) \Omega = 0.02 \text{ S}$ is the characteristic admittance of the probe.

The usable frequency range of the Eq. 17 results from the theory of wave propagation on the microwave transmission line. The incident wave is in TEM mode. The equivalent circuit of the probe consisting of the fringing capacitor is useful for a low frequency range. The higher order modes excited at the discontinuity can be various TM_{0n} modes. The equivalent circuit of the probe consisting of fringing capacitance and radiating conductance is useful in the frequency range above approximately 1 GHz. The range of the operation can be better defined and extended by a field analysis summing a series of TM modes needed to meet boundary conditions at the probe face. TM_{01} is the lowest circular symmetric mode which sharply increases the loss by radiation. Measurement probes are under investigation in the frequency range from 300 kHz (TEM, fringing field) to 3 GHz (TM_{01} , also radiating conductance).

The equivalent circuit has an imperfectly defined range of frequency and permittivity in which a specified uncertainty can be achieved. Equivalent circuits of the probe never take account of the finite MUT sample and finite ground plane flange which give rise to resonances in the response.

The method of solving the complex Eq. 17 consists of splitting it into real and imaginary parts, thereby obtaining a set of two real nonlinear equations for the two real unknowns, which are either C_0 and G_0 (when calibrating the probe) or the real and imaginary part of the complex permittivity ϵ_c of the MUT. To break this down into stages:

- splitting of Eq. 17 into real and imaginary parts
- to obtain C_0 and G_0 , admittance Y for a material with a known complex permittivity ϵ_c (e.g. distilled water) is measured and the set of two equations is solved for the unknowns C_0 and G_0
- to measure of complex permittivity, the admittance Y of a MUT is measured and the set of the two equations is solved for the unknown real and imaginary parts of the ϵ_c

2.4 Modeling and Simulations

An evaluation of this measurement method involves numerical calculation and modeling (Fig. 13). A numerical simulation based on a Finite Integration Technique (FIT, (CST, 2009)) is used to calculate the reflection coefficient on the interface between the probe and the sample of a MUT (Hudlička, 2006). The system that we modeled consists of two parts, i.e. the sensor and the sample of MUT. The modeling is focused on a model with distilled water - the Debye model of distilled water is implemented (Eq. 19). This model was also used for the evaluation of measurement uncertainty.

Choice of Reference Liquid

The material model of distilled water was recognized by Debye in 1926 and describes the complex permittivity of distilled water as a function of frequency.

$$\epsilon_c = \epsilon_r' - j\epsilon_r'' = \epsilon_\infty + \frac{\epsilon_s - \epsilon_\infty}{1 + j\omega\tau} \quad (19)$$

where ϵ_∞ is optical permittivity at high field frequencies, ϵ_s is static permittivity at low field frequencies and τ is electrical relaxation time (a measure of molecules and dipoles mobility). The values of these parameters for distilled water are: $\epsilon_\infty = 4.6$, $\epsilon_s = 78.3$ and $\tau = 8.07$ ps. The condition that a reference material should have similar dielectric properties as the MUT—biological tissue, could not be totally fulfilled because of the very high values of the real part of complex permittivity of biological tissues and their lossy character.

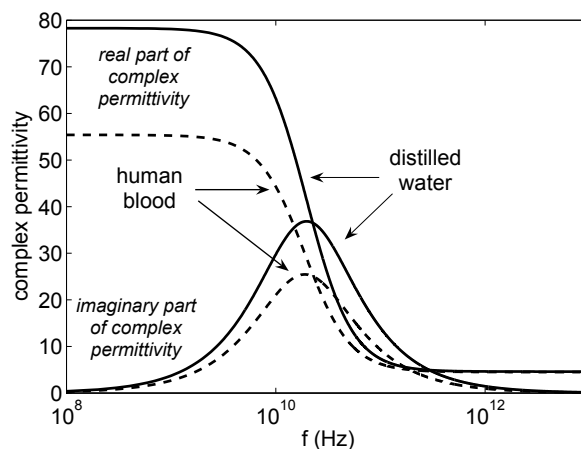


Fig. 12. Dielectric behavior of distilled water and human blood

Fig. 12 shows dielectric properties of the distilled water and the human blood. Distilled water has high values of the real part of complex permittivity and very low values of the imaginary part. Therefore the distilled water is useful reference liquid mainly for the determination of the real part of complex permittivity but neither this condition cannot be satisfied in the whole expected frequency range. Another used reference liquids are alcohols for the dielectric measurements. Unfortunately, an alcohol as a hygroscopic liquid is a time unsteady caliber. Additionally, the dielectric parameters are known from the tables for only 100 % virgin alcohols. Their use in the calibration makes measurements not very precise.

De-embedding the Measurement System

EM field simulation provides information about the reflection coefficient Γ at a reference plane of the excitation port but in order to calculate complex permittivity, the measurement technique needs to obtain the reflection coefficient ($\Gamma_x = S_{11}$) on the interface between the probe and the MUT sample (Fig. 13). In addition, the measurement probe represents an inhomoge-

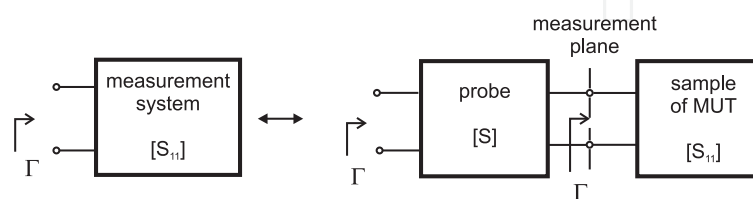


Fig. 13. A model of a reflection coefficient measurement: one-port network (reflection measurement) and the de-embedding of the measurement system

neous transmission line. It is not possible to shift simply the reference plane because of the

different dielectric materials (air and teflon) inside the N connector. It is therefore necessary to perform a de-embedding procedure for the measurement system in order to obtain the correct phase information of the reflection coefficient. Fig. 14 shows the comparison of original data from the numerical modelling and also the measurement with the de-embedded data in the Smith chart. The difference is obvious.

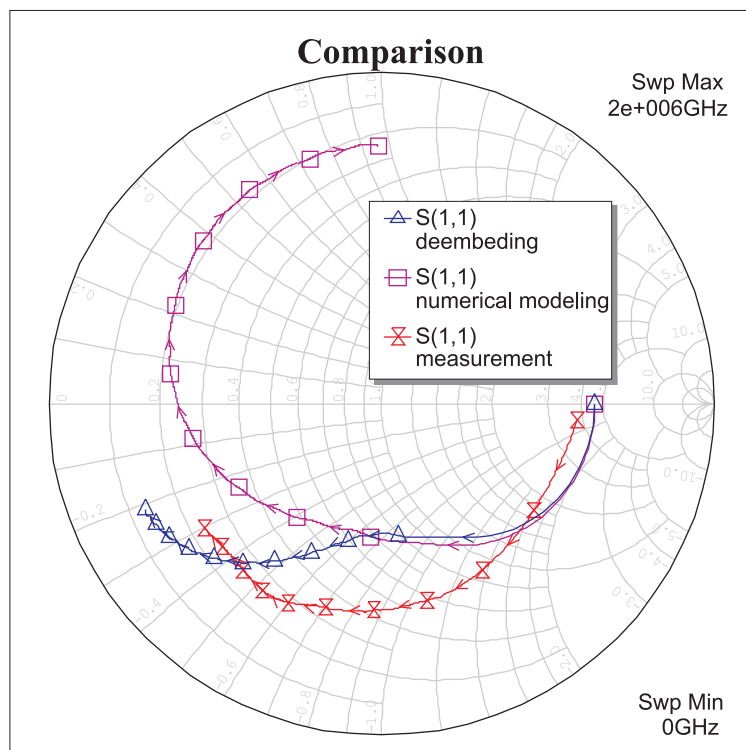


Fig. 14. Comparison of original and de-embedded data: values valid for the agar phantom material

2.5 Measurement System

A typical measurement system using the reflection method on an open-ended coaxial line consists of the network analyzer, the coaxial probe and software. Our measurements (Zajíček, 2009) were done with the aid of an Agilent 6052 network analyzer in the 300 kHz to 3 GHz frequency range. The coaxial probe is placed in contact with a MUT (Fig. 15). Complex permittivity measurement is very fast and proceeds through the three stages. First the calibration of vector network analyzer (VNA) is performed. Then the calibration is carried out using a reference material (with the known dielectric constant ϵ_c). And, finally, the reflection coefficient of MUT is measured. The complex permittivity of MUT is evaluated with the aid of a PC (in our case using MatLab).

2.6 Calibration Kit for Vector Measurement

A calibration kit is a set of physical devices called standards. Each standard has a precisely known or predictable magnitude and phase response as a function of frequency. To be able to

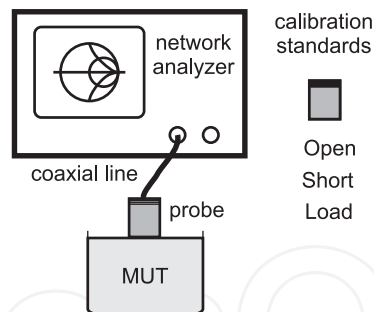


Fig. 15. Measurement system: vector network analyzer, measurement probe and calibration standards for vector measurement

use a particular calibration kit, the known characteristics from each standard in the kit must be entered into the network analyzer memory. The electrical properties of calibration standards

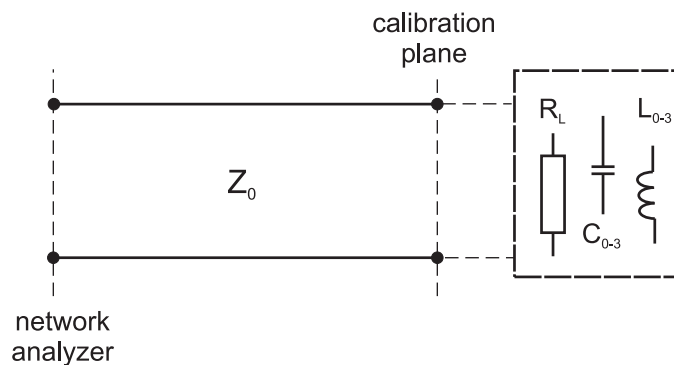


Fig. 16. Specifying the calibration standards

are determined using the modeling in AWR MicroWave Office software. If the actual response of each calibration standard is known (from electromagnetic field solver), then it is possible to determine the value of element in its equivalent circuit (Fig. 16) by tuning this element in order to achieve right (actual) response (Zajíček, 2009).



Fig. 17. Measurement kit: a panel N connector, a measurement probe and open and short calibration standards

The measurement system is a one-port network so the measurement is reduced to measuring the input reflection coefficient S_{11} alone. The OSL (Open, Short and Load) calibration method is performed on the interface between the probe and the MUT sample (reference plane). A coaxial calibration kit was mechanically developed by adapting the panel N and



Fig. 18. Measurement kit: a panel SMA connector, a measurement probe, open, short and matched ($50\ \Omega$) load calibration standards

SMA connectors in the same way as the measurement probe (Fig. 17 and Fig. 18). The short standard is made by the connector which is shorted in the measurement plane by a metal plate. The coaxial open standard is created by two connectors (second one represents the air cavity) and the load standard is a commonly used $50\ \Omega$ termination.

3. Step-by-Step Measurement Procedure

The measurement stages for the MUT are:

- to calibrate the network analyzer
- to measure S_{11} for a substance with a known ϵ_c (distilled water), to compute Y using Eq. 18 and, solving Eq. 17 as outlined above, to determine the constants C_0 and G_0
- to measure S_{11} for any desired MUT, to compute Y (Eq. 18) and to solve Eq. 17 for the unknown real and imaginary part of complex permittivity ϵ_c . Since the equations are of 5th order in terms of ϵ_c , care must be taken to select the physically correct solution (positive real part and negative imaginary part of the ϵ_c)
- if needed, to derive any quantities of interest, such as relative permittivity ϵ_r , loss factor $\tan \delta$ or conductivity σ from the ϵ_c

4. Uncertainty Analysis

The result of dielectric measurement is only an approximation or estimate of the value of the complex permittivity and thus the result is only complete when it is accompanied by a quantitative statement of its uncertainty.

If the measurement device taken to include measurement standards and reference materials is tested through a comparison with a known reference standard and the uncertainties associated with the standard are assumed to be negligible relatively to the required uncertainty of the test, the comparison is viewed as determining the error of the device. The reference standard is the Debye model of distilled water and the standard and combined standard uncertainty of the complex permittivity determination of distilled water is evaluated in the following section.

Sources of an uncertainty are distinguished from the view point of measurement technique. The measurement technique is based on the measurement of the reflection coefficient with the aid of a vector network analyzer. Generally, the calibration of network analyzer and the calibration of measurement probe by means of reference liquid is considered. Last but not least, the condition as a location of coaxial cable which connects the network analyzer with the probe is assumed as a possible contribution to the uncertainty.

This uncertainty evaluation is also the verification of self-consistency of the developed relation between the measured reflection coefficient and the calculated complex permittivity (Eq. 17). Uncertainty evaluation is based on the relevant information available from previous measurement data and experience and knowledge of the behavior and property of the distilled water, and the measurement instruments used (referred to as Type B uncertainty evaluation). Sources of uncertainties and related standard and combined standard uncertainties (Tab. 2 and 3) are evaluated with the aid of guidelines (NIST, 1999).

source of uncertainty	f (MHz)	standard uncertainty (%)
repeated observations	30	0.26
	434	0.29
	915	0.34
random effects	30	4.93
	434	2.16
	915	3.67
systematic effects	30	1.01
	434	0.58
	915	4.50
combined standard uncertainty	30	5.12
	434	2.29
	915	5.90

Table 2. The uncertainty budget, N-type probe: sources of measurement uncertainty are evaluated at important frequencies from a medical point of view

source of uncertainty	f (MHz)	standard uncertainty (%)
repeated observations	434	0.33
	915	0.29
	1800	0.19
	2450	0.37
random effects	434	3.06
	915	2.93
	1800	2.81
	2450	2.14
systematic effects	434	0.58
	915	0.67
	1800	3.69
	2450	20.9
combined standard uncertainty	434	3.19
	915	3.07
	1800	4.72
	2450	21.3

Table 3. The uncertainty budget, SMA-type probe: sources of measurement uncertainty are evaluated at important frequencies from a medical point of view

The applied recommendations given in (NIST, 1999) and mentioned also above are following:

- **Repeatability**

The measurement procedure was performed twenty times over a short period of time (minutes) in a single location with the one-off application of measuring instruments in order to observe the same results.

- **Random Effects**

The measurement procedure was performed ten times over a long period of time (days and months) at a single location with the different application of measuring instruments in order to observe different results. The conditions are generally changed by locating the coaxial cable in a different position between the measurement probe and the network analyzer. The calibration of the network analyzer was performed before each measurement as well as the calibration of the measurement probe by means of distilled water.

It is important to note that complex permittivity is a variable quantity - it changes with frequency, temperature, mixture, pressure and the molecular structure of the MUT. Frequency has a significant influence on changes in the complex permittivity of biological substances. This is the reason for evaluating the uncertainties separately at each frequency of interest for microwave applications.

5. Results

The relative permittivity of lossy materials is a heavily frequency-dependent quantity. Because of the decreasing ability of particles to follow rapid changes of electrical field, the relative permittivity decreases with increasing frequency. The frequencies in the following tables have been selected because of their interest from an industrial, scientific and medical point of view.

5.1 Home-made phantom material

Human tissues can be classified into those with high water content such as muscle, brain, and the internal organs and those with low water content such as fat and bone. The present biological tissue-equivalent phantom⁶ simulates the characteristics of the high-water-content tissues.

ingredients	weight (g)
de-ionized water	3375
agar gelatine	104.6
sodium chloride (NaCl)	37.60
sodium azide (NaN ₃)	2.000
TX-151	84.40
polyethylene powder	337.5

Table 4. The composition of the agar phantom - ingredients for developing a biological muscle tissue-equivalent

⁶ This phantom material was manufactured by Tomáš Dřížďal at the Department of Radiation Oncology, Erasmus MC - Daniel den Hoed Cancer Center, Rotterdam.

The tissue-equivalent phantom can be made of agar, deionized water, polyethylene powder, sodium chloride (NaCl), TX-151, and sodium azide (NaN_3) (Tab. 4). The polyethylene powder is used to adjust the relative permittivity while the conductivity is mainly adjusted by the sodium chloride concentration. Since the agar solution and the polyethylene powder cannot be mixed directly, TX-151 is used to increase the viscosity. Sodium azide is added as a preservative. The advantages of this particular phantom are the ease of use of the original materials and the possibility of manual processing with no need for special production equipment. It is also easy to machine and to cut into arbitrary shapes. The phantom maintains its shape and is mechanically strong. By manipulating the agar, a certain amount of adjustment of the mechanical strength is possible. Hence, this phantom is useful for splitting the phantoms.

f (MHz)	ϵ_r (-)	$\tan \delta$ (-)	σ (S/m)
434	60.9	0.86	1.26
915	58.6	0.54	1.60
1800	53.1	0.47	2.50
2450	48.5	0.48	3.14

Table 5. Dielectric parameters of a home-made muscle tissue phantom

The electrical parameters of the muscle tissue equivalent are described in Tab. 5. Different values of these biological parameters may be required for experimental work. For this reason, it is desirable that the electrical characteristics of the phantom be adjustable within a certain range. In this phantom, the electrical characteristics can be adjusted to a certain extent by modifying the composition shown in Tab. 4. Hence, phantoms are fabricated with varying amounts of polyethylene powder and sodium chloride in order to adjust their permittivity characteristics. To facilitate mixing the polyethylene powder into the agar solution in order to enable the smooth fabrication of the phantom, the amount of TX-151 is dependent on the amount of polyethylene powder. The conductivity is affected by both the polyethylene and sodium chloride whereas the relative permittivity is mainly determined by the polyethylene. Hence, the composition of the phantom with a desired characteristic can be determined first by deriving the amount of polyethylene needed for the desired relative permittivity and then adjusting the conductivity by means of sodium chloride. More details can be found in (Koichi, 2001).

5.2 Commercially available phantom material

This phantom is a tissue-equivalent material, in this case an equivalent of biological muscle tissue. An agar phantom (agar gelatine) is the most commonly used phantom in the testing of thermotherapy applicators, and the use of the phantoms is significant in the measurement of impedance matching and Specific Absorption Rate (SAR).

f (MHz)	ϵ_r (-)	$\tan \delta$ (-)	σ (S/m)
434	57.5 (56.9)	0.31 (0.59)	0.45 (0.81)
915	55.9 (54.9)	0.29 (0.34)	0.85 (0.95)
1800	52.7 (53.5)	0.27 (0.25)	1.42 (1.34)
2450	51.1 (53.5)	0.23 (0.24)	1.63 (1.74)

Table 6. The dielectric parameters of the agar phantom: values of a commercially available phantom DUBLAGA (Zajíček, 2008) and for comparison the values in brackets for muscle tissue (Gabriel, 1999)

The agar phantom is a relatively good equivalent of biological muscle tissue. There is good agreement in the relative permittivity but in the loss factor or conductivity the difference is mainly revealed at lower frequencies (Tab. 6). It appears that the agar has lower water content and is not as lossy as the muscle tissue. If the agar phantom is used, the age of the phantom must be considered.

5.3 Saline phantom

Another type of phantom is a saline liquid (3g of NaCl in 1l of distilled water), simulating biological tissue. A hyperthermia system with the liquid phantom can be used for the evaluation of microwave applicators. This phantom offers 3-D electromagnetic field distribution measurements e.g. the distribution of SAR can be easily calculated with the aid of dipole antennas.

f (MHz)	ϵ_r (-)	$\tan \delta$ (-)	σ (S/m)
434	84.9	0.21	0.57
915	74.4	0.31	1.18
1800	66.4	0.36	2.38
2450	60.2	0.41	3.38

Table 7. Dielectric parameters of saline phantom used in 3-D electromagnetic field distribution measurements

5.4 Melanoma tumor

Another dielectric measurement was performed on an experimental animal with an implanted malignant melanoma. The task was to describe the dielectric properties of the tumor after microwave hyperthermia. In the case of the design of a planar applicator for this experiment

Tissue (measurement)	ϵ_r (-)	$\tan \delta$ (-)	σ (S/m)
tumor (non-invasive)	51.2	0.174	1.21
tumor (invasive)	53.0	0.145	1.05
skin (ex-vivo)	11.1	0.035	0.053

Table 8. Analysis of the dielectric parameters of a melanoma implanted in a mouse

where the dimensions of both animal and tumor are small and care must be taken regarding the effective depth of tissue heating, the dielectric parameters are very important. Tab.

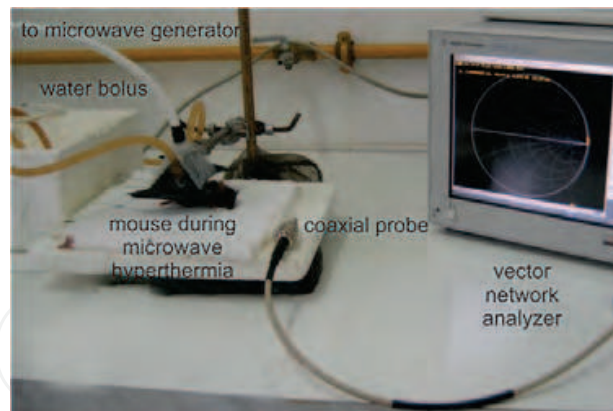


Fig. 19. Microwave hyperthermia: experimental therapy on a laboratory mouse, measurement of the dielectric parameters of an implanted tumor

8 summarizes results measured at a frequency $f = 2.45$ GHz. The tumor dimensions were 30x18 mm. Hyperthermia was applied for a period of 15 minutes with a continual power of 30 W and the achieved temperature in the tumor was 45 °C.

5.5 Biological tissue

Fig. 20 summarizes the values measured on the author's arm and values modeled using a four-layered model of biological tissue. The simulation and the measurement values are based on a model and in vivo sample respectively, these being inhomogeneous (layered). Microwave applicators are usually designed and tested on the agar phantom described in the section below as a homogeneous equivalent of biological muscle tissue. This disparity may affect the impedance matching of microwave applicators. If the complex permittivity of the layered treated area is considered in the design of applicators, a more realistic impedance matching could be achieved.

6. Limitations

Complex relative permittivity is used in calculations of electromagnetic field distribution and is inversely related to the square root in these calculations. This means that the measurement uncertainties from Tab. 2 and 3 are further suppressed. No evaluation of the measurement uncertainties in the case of determining the imaginary part of complex permittivity is presented. For distilled water, this imaginary part has extremely low values (lower than 1) and any evaluation is difficult - there is a high level of uncertainty when is only a small difference between the measured and Debye values.

7. Conclusion

The complex permittivity determination based on reflection coefficient measurement is suitable for the determination of the dielectric parameters of materials in wide bands. This method was described from the viewpoint of electromagnetic field theory and the coaxial probes were described with the equivalent circuit as an antenna in a lossy medium respecting radiation effects at higher frequencies. Some materials were measured and where possible the comparison between measurement (modeling) and values from tables was carried out.

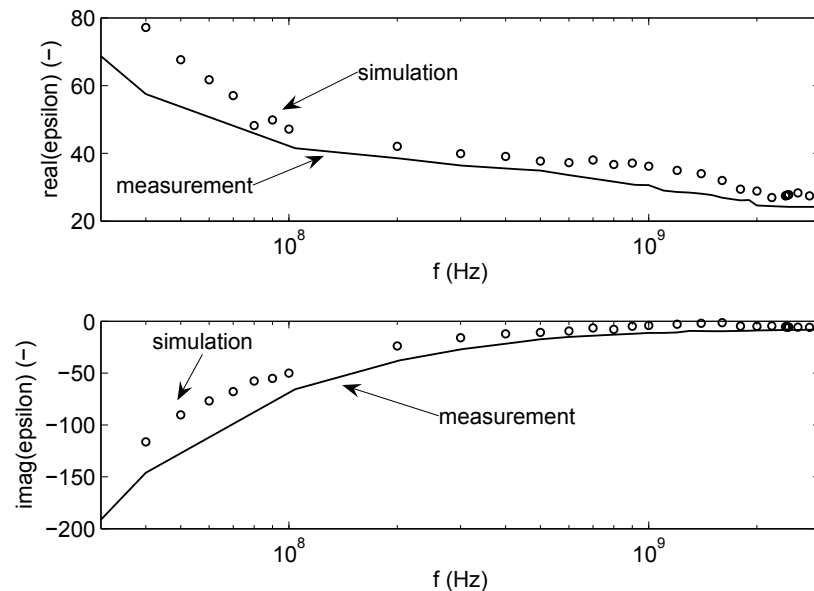


Fig. 20. Complex permittivity measured on author's arm and its comparison with the simulation

Where the evaluation is required to be complete, the uncertainty of measurement has to be specified. The results obtained indicate that the accuracy may be sufficient for most practical applications (2.3-6 % depending on working frequency).

Future perspective of studied method for determining the complex permittivity is in an investigation of layered tissues. Experimental measurement on the layered tissue showed that method yields reasonable approximation of complex permittivity. It could be qualified which range of tissue thicknesses can be considered as sufficient. This would require e.g. statistical analysis of the distribution of the tissue thickness and how they affect the final outcome of the measurement.

8. References

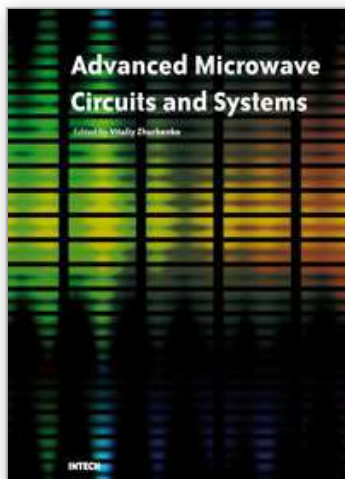
- Deschamps, G., A. (1962). Impedance of an antenna in a conducting medium. *IRE Transactions on antennas and propagation*, p. 648-650.
- Gabriel, C. et al. (1996). The dielectric properties of biological tissues: I. Literature Survey. *Physics in Medicine and Biology*, Vol. 41, p. 2231-2249.
- Hudlička, M., Hazdra, P.: *Finite Integration Technique*. Modeling of Fields. IEEE Czechoslovakia Section, p. 58-77.
- Internet website address: <http://www.p2pays.org/ref/18/17627.pdf> Guidelines for Evaluating and Expressing the Uncertainty of Measurement Results by NIST.
- Internet website address: <http://niremf.ifac.cnr.it/tissprop/> Dielectric properties of body tissues developed by C. Gabriel and colleagues.
- Internet website address: <http://www.cst.com/> CST MW Studio software.
- Kittel, C. (1966). *Introduction to Solid State Physics*, John Wiley&Son, 2nd edition., p. 157-181.
- Koichi I. et al. Development and Characteristics of a Biological Tissue-Equivalent Phantom for Microwaves. *Electronics and Communications in Japan*, Part 1, Vol. 84, No. 4.

- Liu L., X. et al. (1986). Improvement in Dielectric Measurement Technique of Open-ended Coaxial Line Resonator Method. *Electronics Letters*, Vol. 22, No. 7, p. 373-375.
- Novotný, K. (2005). *Theory of Electromagnetic Field*, Press CTU in Prague.
- Novotný, K. (2001). *Theory of Electromagnetic Field II: Field and Waves*, Press CTU in Prague.
- Stuchly M., A. et al. (1982). Measurement of RF permittivity of biological tissue with an open-ended coaxial line: Part II-Experimental results. *IEEE transactions on MTT*, Vol. 30, no.1, p. 82-92.
- Vrba, J. (2003). *Medical applications of microwave technique*, Press CTU in Prague, p. 46-61.
- Zajíček, R. et al. (2008). Broadband Measurement of Complex Permittivity Using Reflection Method and Coaxial Probes. *Radioengineering*, Vol. 17, No. 1, p. 14-19, ISSN 1210-2512.
- Zajíček, R. (2009). *Application of Complex Permittivity in Medical Diagnostics and Imaging*, Doctoral Thesis, CTU in Prague.

IntechOpen

IntechOpen

IntechOpen



Advanced Microwave Circuits and Systems

Edited by Vitaliy Zhurbenko

ISBN 978-953-307-087-2

Hard cover, 490 pages

Publisher InTech

Published online 01, April, 2010

Published in print edition April, 2010

This book is based on recent research work conducted by the authors dealing with the design and development of active and passive microwave components, integrated circuits and systems. It is divided into seven parts. In the first part comprising the first two chapters, alternative concepts and equations for multiport network analysis and characterization are provided. A thru-only de-embedding technique for accurate on-wafer characterization is introduced. The second part of the book corresponds to the analysis and design of ultra-wideband low-noise amplifiers (LNA).

How to reference

In order to correctly reference this scholarly work, feel free to copy and paste the following:

Radim Zajicek and Jan Vrba (2010). Broadband Complex Permittivity Determination for Biomedical Applications, *Advanced Microwave Circuits and Systems*, Vitaliy Zhurbenko (Ed.), ISBN: 978-953-307-087-2, InTech, Available from: <http://www.intechopen.com/books/advanced-microwave-circuits-and-systems/broadband-complex-permittivity-determination-for-biomedical-applications>

INTECH
open science | open minds

InTech Europe

University Campus STeP Ri
Slavka Krautzeka 83/A
51000 Rijeka, Croatia
Phone: +385 (51) 770 447
Fax: +385 (51) 686 166
www.intechopen.com

InTech China

Unit 405, Office Block, Hotel Equatorial Shanghai
No.65, Yan An Road (West), Shanghai, 200040, China
中国上海市延安西路65号上海国际贵都大饭店办公楼405单元
Phone: +86-21-62489820
Fax: +86-21-62489821

© 2010 The Author(s). Licensee IntechOpen. This chapter is distributed under the terms of the [Creative Commons Attribution-NonCommercial-ShareAlike-3.0 License](#), which permits use, distribution and reproduction for non-commercial purposes, provided the original is properly cited and derivative works building on this content are distributed under the same license.

IntechOpen

IntechOpen